Oscillatory Dissipation of a Simple Confined Liquid

Abdelhamid Maali,* Touria Cohen-Bouhacina, Gérard Couturier, and Jean-Pierre Aimé
CPMOH, Université Bordeaux1, 351 Cours de la Libération, 33405 Talence, France
(Received 31 October 2005; published 3 March 2006)

We present a sensitive measurement of the dissipation and the effective viscosity of a simple confined liquid (octamethylcyclotetrasiloxane) using an atomic force microscope. The experimental data show that the damping and the effective viscosity increase and present oscillations as the gap between the cantilever tip and the surface is diminished. To our knowledge, the damping and the viscosity modulation are reported here with such good accuracy for the first time. Such an experimental result is different from what has been reported earlier where only a continuous increase of the damping and the viscosity are observed.

DOI: 10.1103/PhysRevLett.96.086105 PACS numbers: 68.08.−p, 68.15.+e, 68.37.Ps

The physical properties of materials at the nanometer scale can be completely different from those of the bulk. A good example of this is provided by a liquid at a solid interface in which the liquid undergoes some ordering due to the presence of interactions with the solid wall. Ordering of liquids at interfaces is a phenomenon of fundamental importance and has interested several fields of research such as tribology [1], nanofluidics [2], and biology [3]. It has been extensively studied using the surface force apparatus (SFA) [2–11] and atomic force microscopy (AFM) [12–20].

Several pioneering works [2–18,20] reported that the solvation force (force acting on surfaces confining a fluid) has an oscillatory profile versus the distance separating the surfaces. Moreover, the viscosity measured by shearing the confining surfaces laterally was reported to increase strongly with the decreasing thickness of the confined liquid [5,6,8–11]. However, the modulation behavior of the viscosity and damping which we report here has been measured directly and with such high accuracy for the first time. In previous AFM experiments on confined liquids [12–18,20], researchers used either tapping mode or frequency modulation mode. Those used tapping mode worked at subresonance frequency [12–18], which results in lower sensitivity of the phase signal, and those working in frequency modulation mode used amplitudes in the range of 2–7 nm [20], which induces an averaging of the measured signal over the motion of the cantilever tip. Furthermore, due to the height of the cantilever tip used in some experiments [14,16], the fluid is squeezed between the cantilever and the surface, resulting in a large viscous hydrodynamic force acting on the cantilever and opposing the motion. This viscous damping effect reduces the AFM sensitivity when working in the dynamic mode and measuring the phase and the amplitude. As a result of this lack of sensitivity, the modulation of the damping has never been clearly observed.

In the work presented here, the experiments were performed in tapping mode and close to the cantilever resonance frequency in order to increase the sensitivity. In contrast to earlier AFM tapping mode experiments on confined liquids, in which the frequencies used are in the range or below 1 kHz, the working frequency is about 31 kHz in our experiments. Therefore, for the same integration time, many more measurements are averaged, increasing the signal to noise ratio. Additionally, cantilevers with high tips (15 μm) were used in order to minimize the contribution of the squeezed fluid between the cantilever and the surface that induces additional bulk dissipation [21].

For a cantilever oscillating with a small amplitude compared to the range of the interaction length which, in our case, is roughly the size of the molecule or the oscillation period, the force induced by the confined fluid has two contributions; one is a conservative term ($-k_{\mathrm{int}}z$), and the other is a dissipative term ($-\gamma_{\mathrm{int}}\dot{z}$), where k_{int} and γ_{int} are the effective interaction stiffness and damping coefficient of the confined liquid, respectively, and z is the instantaneous position of the cantilever. The motion of the cantilever is then described by:

$$m^*\ddot{z} + (\gamma_0 + \gamma_{\mathrm{int}})\dot{z} + (k_l + k_{\mathrm{int}})z = F_0 \exp(j\omega t). \quad (1)$$

With the driving force $F_0 = k_l A_0/Q$, m^* is the effective mass of the cantilever and γ_0 is the viscous hydrodynamic damping far from the surface and is related to the quality factor Q and the resonance frequency ω_0 via the equation $Q = m^*\omega_0/\gamma_0$. k_l is the cantilever stiffness and A_0 is the amplitude of the oscillation far away from the interaction region. The stationary solution $z = A\exp j(\omega t + \varphi)$ of the above equation gives the stiffness and the damping coefficient:

$$k_{\mathrm{int}} = k_l\left(\frac{A_0\cos(\varphi)}{AQ} - 1 + \frac{\omega^2}{\omega_0^2}\right) \quad (2)$$

and

$$1 + \gamma_{\mathrm{int}}/\gamma_0 = -\frac{\omega_0 A_0}{\omega A}\sin(\varphi), \quad (3)$$

where A and φ are, respectively, the measured amplitude and phase of the oscillation, and ω is the driving frequency of the cantilever.

The data presented in this Letter are obtained using a MikroMasch cantilever with a resonance frequency in liquid of 32.2 kHz and a quality factor Q of 3.7. The

nominal tip radius is 10 nm and the spring constant is $k_l = 0.95$ N/m. The cantilever is vibrated at amplitudes ranging from 0.8 to 3.2 angstroms. The liquid confined between the tip and a freshly cleaved surface of highly oriented pyrolytic graphite is octamethylcyclotetrasiloxane (OMCTS) purchased from Sigma and used as received. The experiments were performed in ambient air at room temperature using a commercial AFM (NanoScope III-extended Multimode, Veeco Instruments). The vibrating amplitude and phase are measured using a lock-in amplifier (Stanford RS830), and the output data are stored with a digital oscilloscope TDS 3032 (10 000 points/channel memory). The data are obtained by varying the tip-sample separation and recording the vibration amplitude and phase of the cantilever. In each cycle, the tip is approached at a velocity of 1 nm/s until the amplitude drops to zero (touching the surface), and then the tip is retracted at the same velocity. In our experiment, the thermal drift was about 0.3 Å/s. Figure 1 shows the schematic of the cantilever tip confining the fluid. The cantilever tip is vibrated at a very small amplitude, and, at each average tip-surface gap, we measured the phase and amplitude of the cantilever.

Figure 2 presents the amplitude (A) and phase (B) recorded as the tip approaches the surface. We can clearly observe several oscillations in the curves. The oscillation period is nearly independent of the amplitude of the cantilever-tip vibration. The average periodicity measured over 20 approach-retract cycles is 7.8 angstroms [Fig. 2(c)], which is consistent with values previously reported using SFA for OMCTS on mica [7] and AFM for OMCTS on graphite [14]. The interaction is varying on a length equal to the period of the modulation of the amplitude and phase curves. The modulation contrast in the amplitude and the phase curves is reduced as the cantilever amplitude is increased. To satisfy the condition of small amplitudes, one should further reduce the amplitude, which requires a large integration time in the lock-in amplifier and, thus, a low velocity in the approach-retract curves. However, this induces a large contribution of the thermal drift. We have found that, to obtain a good signal to noise ratio with a small integration time (to minimize the thermal drift contribution), one has to use amplitudes not smaller than 0.8 Å. The smallest amplitude used in the presented data (0.8 Å) is 10 times smaller than the typical oscillation length, and thus the approximation of small amplitudes is satisfied and Eqs. (2) and (3) are valid.

Using Eqs. (2) and (3), we convert amplitude and phase data to get the interaction stiffness and the damping coefficient for the cantilever amplitude of 0.8 Å. For larger amplitudes, we have to use more sophisticated calculations similar to those developed for frequency modulation atomic force microscopy [20,22,23], in order to get accurate values of the stiffness from the measured amplitude and phase values since the approximation of small amplitude is not valid. Figure 3 presents the interaction stiffness versus tip-substrate distance. Similarly to the phase and amplitude curves, we can clearly see the modulation of the stiffness with a periodicity equal to the molecular diameter. The maxima of the interaction stiffness correspond to situations in which the liquid is denser than the bulk and the cantilever senses a force pushing the tip as it enters the layer. The zero values correspond to situations in which the liquid density is similar to that of the bulk. The minima of the stiffness correspond to situations in which the fluid

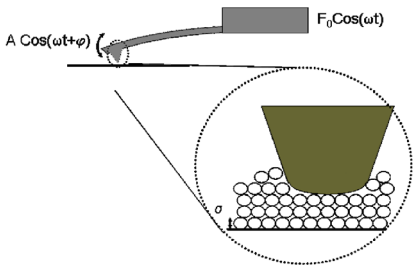

FIG. 1 (color online). Schematic representation of the experiment. The cantilever was driven at fixed forcing, and we measured simultaneously the phase and the amplitude of the cantilever as the tip approaches the surface.

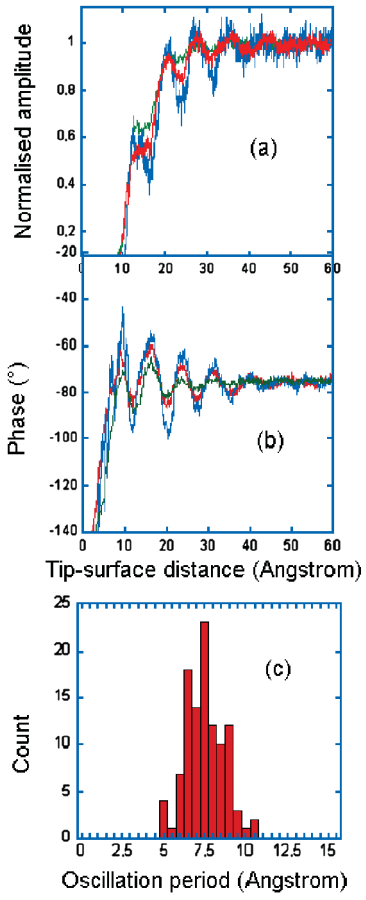

FIG. 2 (color). (a) Amplitude and (b) phase of the cantilever as the tip approach to the surface for differents amplitude: blue line, $A_0 = 0.8$ Å; red line, $A_0 = 1.6$ Å; and green line, $A_0 = 3.2$ Å. (c) Histogram of the measured oscillation period in the amplitude signal.

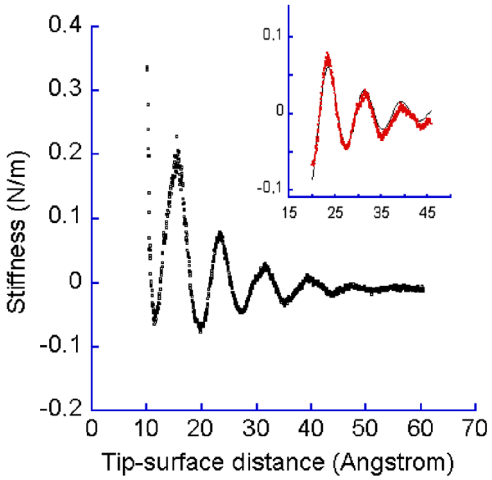

FIG. 3 (color online). The interaction stiffness versus the gap between the cantilever tip and the substrate. The inset shows the best fit of three periods of the modulated stiffness.

density below the tip is smaller than the bulk density, thus inducing a force over the tip motion. The explanation of the variation of the stiffness by a variation of the density is supported by recent work [24], in which density fluctuations induced by confinement has been reported using an improved SFA apparatus.

From SFA experiments [7], the solvation force per unit area acting between two flat surfaces has an oscillatory profile which decays exponentially and can be approximated by:

$$f(D) \approx p_0 \cos(2\pi D/\sigma) \exp(-D/\tau), \quad (4)$$

where D is the distance between the two surfaces, σ is the molecular diameter [$\sigma = 0.78$ nm, Fig. 2(c)], and τ is the decay length of the interaction. The decayed oscillatory profile of the solvation force has also been obtained by several authors using molecular dynamics simulations [25,26].

By summing f over the surface of the spherical tip of radius R, we get the total force F acting on the cantilever tip and, thus, the interaction stiffness (the gap D is assumed small compared to R):

$$k_{\text{int}}(D) = -\frac{\partial F}{\partial D} = p_0 2\pi R \cos(2\pi D/\sigma) \exp(-D/\tau). \quad (5)$$

The above expression is oversimplified, but it reproduces the main experimental observations, i.e., the oscillatory variation of the stiffness and the exponential decay profile. Notice that, unlike in SFA experiments, the radius of the AFM tip is not infinite compared to the molecular diameter. The accurate expression of the stiffness should take into account the van der Waals term that is a difficult task due to the density modulation of the confined liquid. The contribution of the van der Waals interaction to the value of the effective stiffness is important only when the tip is close to the surface. Thus, we consider only the third, fourth, and fifth measured periods of the stiffness to fit our experimental data to Eq. (5). The molecular diameter is assumed constant and is determined from the histogram in Fig. 2(c); $\sigma = 0.78$ nm. We have found $\tau = 11.2$ Å, $2\pi R p_0 = 0.51$ N/m. The decay length $\tau = 11.2$ Å is equal to 1.44σ, which is consistent with results reported earlier [7] (decay length of 1.2–1.7σ). With a tip radius $R = 10$ nm, we get $p_0 = 8.1$ MPa. Notice that the value of p_0 is not different from that calculated by the expression $p_0 \approx k_B T \rho$ [7], where k_B is the Boltzmann constant, ρ is the molecular density, and T is the temperature, for OMCTS at room temperature $p_0 = 7.8$ MPa.

Figure 4 shows the damping versus the distance between the cantilever tip and the surface. For distances greater than 50 angstroms, the interaction damping is zero. As the tip approaches the surface, the damping shows two features: a periodic variation and an increase. The damping modulation period is equal to the molecular diameter. Notice that the damping is in phase with the stiffness curve (dashed line). When the tip-surface distance is equal to a multiple of the molecular diameter (distances corresponding to the maxima of the stiffness), the damping is higher, and, for distances corresponding to a multiple and half of the diameter, the damping is at minimum.

If we assume a constant fluid viscosity equal to the bulk viscosity ($\eta = 2.2$ cPs), the nonslip boundary conditions [27] combined with the Navier-Stokes equation give the Reynolds force acting on the cantilever tip, at the first order:

$$F = \frac{6\pi\eta R^2}{D} \frac{dD}{dt}, \quad (6)$$

where R is the tip radius and D is the gap between the tip

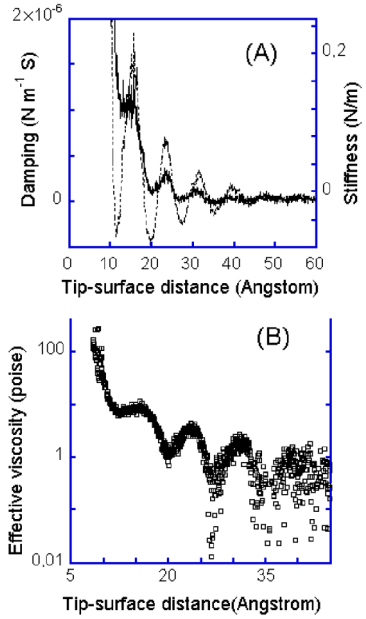

FIG. 4 (color online). (a) Measured damping of the confined liquid versus the tip-surface gap. (b) Effective viscosity as the tip approaches the surfaces extracted from the data of the damping.

and the surface. The temporal variation of the tip-surface gap is equal to the velocity of the cantilever. Therefore, the hydrodynamic damping coefficient is

$$\gamma_{\mathrm{Hydro}} = F/(dD/dt) = \frac{6\pi\eta R^2}{D}.$$

One can compare this hydrodynamic damping to the measured damping. At 1 nm far from the surface and with a tip radius $R = 10\,\mathrm{nm}$, $\gamma_{\mathrm{Hydro}} = 4.2 \times 10^{-9}\,\mathrm{N\,m^{-1}\,S}$, $\gamma_{\mathrm{int}} = 2 \times 10^{-6}\,\mathrm{N\,m^{-1}\,S}$. Assuming a constant value of the viscosity ($\eta = 0.022$ Ps) leads to very small dissipation ($\gamma_{\mathrm{Hydro}}/\gamma_{\mathrm{int}} = 0.002$). The increase of the damping cannot be described by a hydrodynamic force acting on the cantilever tip moving in a fluid behaving like a bulk fluid with a constant viscosity. Klein, Granick, and others reported an increase of viscosity of confined OMCTS [8–11]. Their measurements are based on shearing the SFA confining surface laterally and measuring the frictional force. In the SFA experiment during the approach, the surfaces separations D for a film of thickness $n\sigma$ are measured only from $n\sigma$ to $(n + 1/2)\sigma$. The distance range $(n + 1/2)\sigma < D < (n + 1)\sigma$ is not accessible because of the finite spring constant of the apparatus. Also due to a limited number of measurements versus the surfaces gap in those experiments, they reported only an increase of viscosity. In our experiment, we have access to a nearly continuous tip-surface gap variation. The gap is varied with a step of 0.04 Å. For each cantilever-tip-surface distance, the confined liquid can be described by a fluid having an effective viscosity

$$\eta_{\mathrm{eff}} = \frac{\gamma_{\mathrm{int}} D}{6\pi R^2}.$$

The effective viscosity extracted from the damping data is shown in Fig. 4(b). The viscosity is not only increasing as reported earlier in SFA experiments but is also modulated. The viscosity modulation length is equal to the molecular diameter. The uncertainty of the measurements is of the order of 0.1 poise, which is sufficient to show the modulation of the viscosity. For films of thickness corresponding to one monolayer, the viscosity is larger than 200 poise, which is 4 orders of magnitude larger than the bulk viscosity. Notice here that, in contrast to SFA experiment where one measures shear stress and derives the viscosity by assuming the couette flow geometry, the viscosity is measured here by normal approaching the tip to the surface.

In summary, we have presented measurements on a simple confined liquid using an atomic force microscope in the tapping mode. In addition to the oscillations in the stiffness curve, our experimental data also show the modulation of the damping and viscosity as the tip approaches the surface. To our knowledge, the damping and viscosity modulations are reported here with such good accuracy for the first time. The quality of the recorded experimental data gives one the opportunity to investigate accurately the structure and companion rheological properties of confined liquid as a function of boundary conditions. In particular, we should be able to investigate liquid confinement at proximity of F1 proteins assembly of ATP synthase, the basic aim being to investigate the role of confined liquid on its ability to monitor the enzyme substrate interaction.

The authors thank C. Hurth and R. Boisgard for reading of the manuscript and H. Kellay, A. Würger, P. Richetti, and C. Drummond for helpful discussions.

*Electronic address: a.maali@cpmoh.u-bordeaux1.fr

[1] B. N. J. Persson, *Sliding Friction: Physical Principles and Applications* (Springer, Heidelberg, 2000), 2nd ed.
[2] T. Becker and F. Mugele, Phys. Rev. Lett. **91**, 166104 (2003).
[3] J. Israelachvili and H. Wnnerström, Nature (London) **379**, 219 (1996).
[4] R. G. Horn and J. Israelachvili, J. Chem. Phys. **75**, 1400 (1981).
[5] M. L. Gee, P. M. McGuiggan, and J. N. Israelachvili, J. Chem. Phys. **93**, 1895 (1990).
[6] S. Granick, Science **253**, 1374 (1991).
[7] J. Israelachvili, *Intermolecular and Surfaces Forces* (Academic, London, 1992).
[8] J. Klein and E. Kumacheva, J. Chem. Phys. **108**, 6996 (1998).
[9] E. Kumacheva and J. Klein, J. Chem. Phys. **108**, 7010 (1998).
[10] E. Kumacheva and J. Klein, Science **269**, 816 (1995).
[11] A. L. Demirel and S. Granick, Phys. Rev. Lett. **77**, 2261 (1996).
[12] S. J. O'Shea, W. E. Welland, and J. B. Pethica, Chem. Phys. Lett. **223**, 336 (1994).
[13] W. Han and S. M. Lindsay, Appl. Phys. Lett. **72**, 1656 (1998).
[14] R. Lim, S. F. Y. Li, and S. J. O'Shea, Langmuir **18**, 6116 (2002).
[15] R. Lim and S. J. O'Schea, Phys. Rev. Lett. **88**, 246101 (2002).
[16] R. Y. H. Lim and S. J. O'Shea, Langmuir **20**, 4916 (2004).
[17] M. Antognozzi, A. D. L. Humphris, and M. J. Milles, Appl. Phys. Lett. **78**, 300 (2001).
[18] S. Jeffery *et al.*, Phys. Rev. B **70**, 054114 (2004).
[19] J. P. Cleveland, T. E. Schäffer, and P. K. Hansma, Phys. Rev. B **52**, R8692 (1995).
[20] T. Uchihashi, Appl. Phys. Lett. **85**, 3575 (2004).
[21] O. I. Vinogradova and G. E. Yakubov, Langmuir **19**, 1227 (2003).
[22] F. J. Giessibl, Appl. Phys. Lett. **78**, 123 (2001).
[23] J. E. Sader and S. P. Jarvis, Appl. Phys. Lett. **84**, 1801 (2004).
[24] M. Heuberger, M. Zäch, and N. D. Spencer, Science **292**, 905 (2001).
[25] J. Gao, W. D. Luedtke, and U. Landman, Phys. Rev. Lett. **79**, 705 (1997).
[26] P. Bordarier, B. Rousseau, and A. Fuchs, J. Chem. Phys. **106**, 7295 (1997).
[27] The deviation from the nonslip boundary condition can be quantified by a dimensionless function $f^* \leq 1$ [O. I. Vinogradova, Langmuir **11**, 2213 (1995)]. Then the Reynolds equation becomes $F_{\mathrm{Hydro}} = f^*(6\pi\eta R^2/D)(dD/dt)$ and the hydrodynamic damping becomes $\gamma_{\mathrm{Hydro}} = f^*(6\pi\eta R^2/D)$.